

Soft-template-assisted Synthesis of Hierarchical NiCo₂O₄ array /Ni foam for application in supercapacitors

Zhouli Hui¹, Shushan Yao², TaiKan Ou¹, Qingxiao Liu¹, Lifei Zhi³, Yang Cao¹, Youyi Sun^{1*}

¹ School of Material Science and Engineering, North University of China, Taiyuan, Shanxi Province. 030051, China.

² School of Materials Science and Engineering, Taiyuan University of Science and Technology, Taiyuan 030024, Shanxi, P. R. China.

³ School of Chemical and Biological Engineering, Taiyuan University of Science and Technology, Taiyuan 030024, Shanxi, P. R. China.

*E-mail: syyi@pku.edu.cn (YY. Sun).

Received: 8 December 2021 / Accepted: 16 January 2022 / Published: 4 March 2022

The hierarchical NiCo₂O₄ array structure/Ni foam (NiCo₂O₄/NF) is prepared by a soft-template-assisted hydrothermal approach for application in supercapacitors. Furthermore, the micro-structure of porous NiCo₂O₄ nanoarray on Ni foam can be easily tuned by reaction time under assistance of quaternary ammonium gemini surfactant. The electrochemical properties of NiCo₂O₄ array on Ni foam with various morphologies are also investigated and compared. Among them, the NiCo₂O₄ nanofiber array shows the better performance comparing to other counterparts, such as a larger area capacitance of 2.89 F cm⁻² and excellent cycling stability, maintaining *ca.* 87.9% of its initial capacitance after 2000 cycles. This work provides a facile way to prepare hierarchical porous NiCo₂O₄ array grown on Ni foam for various applications.

Keywords: NiCo₂O₄; Ni foam; chemical synthesis; soft template; supercapacitor.

1. INTRODUCTION

Supercapacitor has attracted lots of attentions due to long cycle life, high power density and environmental friendly[1]. The performance of supercapacitors is mainly determined by the structure and properties of the electrode[2]. Recently, NiCo₂O₄/Ni foam (NiCo₂O₄/NF) was developed for application in electrodes of supercapacitor due to low interface resistance, low internal resistance and large active surface area [3]. For example, Wang et al reported the synthesis of NiCo₂O₄ grown on Ni foam by a facile hydrothermal method, in which the morphology was controlled by adjusting the content of NH₄F[4]. Zheng et al reported the synthesis of hierarchical porous NiCo₂O₄ grown on Ni foam by a

facile hydrothermal method[5]. Wang et al reported the synthesis of various NiCo_2O_4 arrays grown on Ni foam by a facile hydrothermal method, which were controlled by introduction of chemical reaction reagent (alkali source and NH_4F)[6]. Liu et al reported the synthesis of porous NiCo_2O_4 nanoneedle array grown on Ni foam by a facile pulsed laser ablation (PLA) approach[7]. Shim et al reported the synthesis of NiCo_2O_4 array grown on Ni foam by a simple combustion method [8]. Zhang et al reported the synthesis of NiCo_2O_4 nanosheet array grown on Ni foam by the electrodeposition method followed thermal treatment[9]. Li et al reported the synthesis of hierarchical NiCo_2O_4 arrays (eg. 1D nanowires and 2D nanosheets) grown on Ni foam by combing hydrothermal method with annealing process[10]. Liu et al prepared the hierarchical $\text{NiCo}_2\text{O}_4/\text{Ni}$ foam by combing hydrothermal method with annealing process[11]. Xue et al prepared $\text{NiCo}_2\text{O}_4/\text{Ni}$ foam by the hydrothermal method[12]. Although there are some works reporting the synthesis of various NiCo_2O_4 arrays grown on Ni foam, yet, these micro-structure of NiCo_2O_4 are mainly controlled by the reaction conditions, such as content of NH_4F , alkali source and so on. In addition, these NiCo_2O_4 arrays grown on Ni foam are prepared by a free-template method, in which the micro-structure is high sensitivity to these reaction conditions. So it is still a high challenge to control the micro-structure of NiCo_2O_4 arrays on Ni foam. As well-known, metal oxide materials can be controllable synthesis by a soft-template method, in which the micro-structure (eg morphology and size) can be easily tuned[13]. As well-known, quaternary ammonium gemini surfactant can form micelles with various morphologies, which is a good kind of soft-template for controlling synthesis of metal oxide[14]. However, up to now, the preparation of NiCo_2O_4 array grown on Ni foam are few reported by the soft-template based on quaternary ammonium gemini surfactant for application in electrodes of supercapacitor.

Here, the $\text{NiCo}_2\text{O}_4/\text{NF}$ electrodes were facilely prepared by a soft-template based on quaternary ammonium gemini surfactant. The micro-structure of NiCo_2O_4 array grown on Ni foam can be easily adjusted by controlling the reaction time under assistance of surfactant. Furthermore, the effect of NiCo_2O_4 structures on the properties of the $\text{NiCo}_2\text{O}_4/\text{NF}$ was also investigated in detail. The $\text{NiCo}_2\text{O}_4/\text{NF}$ exhibited good electrochemical performance. This work proves a controlled method to prepare the $\text{NiCo}_2\text{O}_4/\text{NF}$ electrode with various structures for various applications.

2. EXPERIMENTS

2.1 Preparation of $\text{NiCo}_2\text{O}_4/\text{NF}$

The Ni foam (NF) was treated by HCl (3.0mol/L) and then washed by ethanol and water under ultrasonic for 30min. The treated NF, 1.32 mmol $\text{Co}(\text{NO}_3)_2 \cdot 6\text{H}_2\text{O}$, 0.366 mmol $\text{Ni}(\text{NO}_3)_2 \cdot 6\text{H}_2\text{O}$, 20.0 mmol urea, 8.0 mmol NH_4F and 0.05g N,N-dimethyl dodecyl/tetradecyl tertiary amine quaternary ammonium gemini surfactant (G-CA) were added to 40.0mL aqueous solution. The above mixture was added to autoclave. The autoclave was treated at 180.0°C for various times (4.0 h, 6.0 h, 8.0 h and 10.0 h) and then cooled down to room temperature. The product based on NF was took out from autoclave and dried at 60.0°C . Finally, the product was further calcination at 300°C for 2h, forming $\text{NiCo}_2\text{O}_4/\text{NF}$.

2.2 Characterization

The crystal structure of NiCo₂O₄/NF was characterized by the X-ray diffractometer. The average size of NiCo₂O₄ particles was calculated by equation (1).

$$D=57.3 \cdot K \cdot \lambda / \beta \cdot \cos \theta \quad (1)$$

Where, D (nm), λ (nm), β and θ are the diameter of particles, radiation wavelength, and the fullwidth at half and Bragg angle, respectively.

The micro-structure of NiCo₂O₄/NF was characterized by the Scanning Electron Microscopy (SU-8100).

Cyclic voltammetry (CV) and electrochemical impedance spectroscopy (EIS) were characterized by a workstation (CHI 660D) in 6.0 M KOH solution. Here, Hg/Hg₂Cl₂, the platinum wire and NiCo₂O₄/NF acted as the reference, counter and working electrode, respectively. The electrochemical active surface area (ECSA, C cm⁻²) was calculated according to equation (2).

$$ECSA = \frac{S_H / V}{0.21(C \cdot cm^{-2}) \cdot M} \quad (2)$$

Where, V (mV s⁻¹), M (cm²) and S_H (A V) are the scan rate, area of active material and integral area of CV curve, respectively.

The galvanostatic charge/discharge (GCD) curves were characterized by workstation (CHI 660D). The area capacitance (C_A , F cm⁻²) was obtained according to equation (3).

$$C_A = I \cdot \Delta t / S \cdot \Delta U \quad (3)$$

The S (cm²), ΔU (V), I (A) and Δt (s) are the area of the electrode, the potential change, current and time, respectively.

3. RESULTS AND DISCUSSION

Fig.1 showed the XRD spectra of products. Three strong diffraction peaks of 44.8°, 52.3° and 76.5° were observed, corresponding to the (111), (200) and (220) crystal planes of Ni metal (JCPDS card No.04-0850), respectively[15]. In addition, some new diffraction peaks of 19.0°, 31.4°, 36.8°, 59.7° and 62.8° were also observed, which were assigned to the (111), (220), (311), (511) and (440) crystal planes of NiCo₂O₄ (JCPDS card No. 73-1702)[11]. In addition, the diffraction peaks of NiCo₂O₄ increased with increasing in reaction time. The result was attributed to more load of NiCo₂O₄ grown on Ni foam prepared at longer reaction time. According to the Debye-Scherrer equation, the average sizes of the NiCo₂O₄ crystal were further calculated to be 12.6 nm, 7.5nm, 7.6 nm and 8.1 nm for the NiCo₂O₄ prepared at various reaction times of 4.0 h, 6.0 h, 8.0 h and 10.0 h, respectively. These results confirmed the formation of NiCo₂O₄ grown on NF by present process.

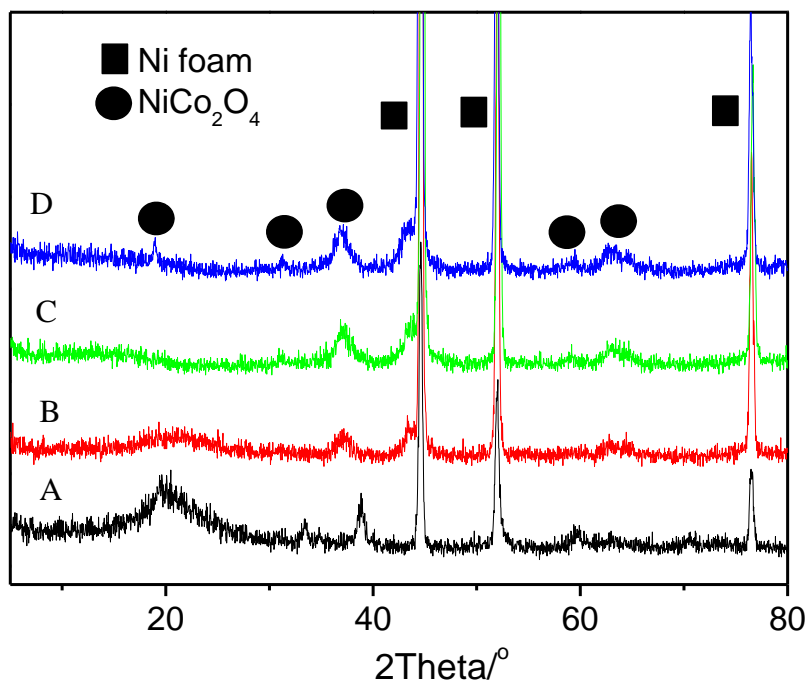


Figure 1. XRD patterns of $\text{NiCo}_2\text{O}_4/\text{NF}$ prepared at various reaction times, (A) 4.0h, (B) 6.0h, (C) 8.0h and (D) 10.0h.

The micro-structures of the $\text{NiCo}_2\text{O}_4/\text{NF}$ prepared at various reaction times were further characterized by the SEM images in Fig.2. The pure NF showed silvery (inset of Fig.2A), which changed to black after chemical reaction (inset of Fig.2B), indicating the formation of $\text{NiCo}_2\text{O}_4/\text{NF}$ [16]. As shown in Fig.2A-D, we observed that the surface of the foam's skeleton became rough and no particles were formed in the holes. This result further indicated that the NiCo_2O_4 was grown on skeleton of NF, forming porous foam structure. Fig.2E-H showed the magnification images of the $\text{NiCo}_2\text{O}_4/\text{NF}$ prepared at various reaction times. It was found that the micro-structure of NiCo_2O_4 grown on NF strongly depended on reaction times. All samples showed flake array structure. The NiCo_2O_4 flake array prepared at longer reaction time showed denser and smaller. Furthermore, the NiCo_2O_4 flake array prepared at 8.0h and 10.0h showed similar hierarchical structure, which was composed of nanofiber and nano-needle, respectively. The hierarchical micro-structure composed of nanosheets and nanofibers has been few observed, in which it was generally sheet array[7, 9-10]. In a comparison, the size of NiCo_2O_4 nanofiber prepared at 8.0h was smaller comparing to the NiCo_2O_4 nano-needle prepared at 10.0h. These results confirmed the formation of $\text{NiCo}_2\text{O}_4/\text{NF}$ with various micro-structure, which were easily tuned under assistant of G-CA by controlling reaction time.

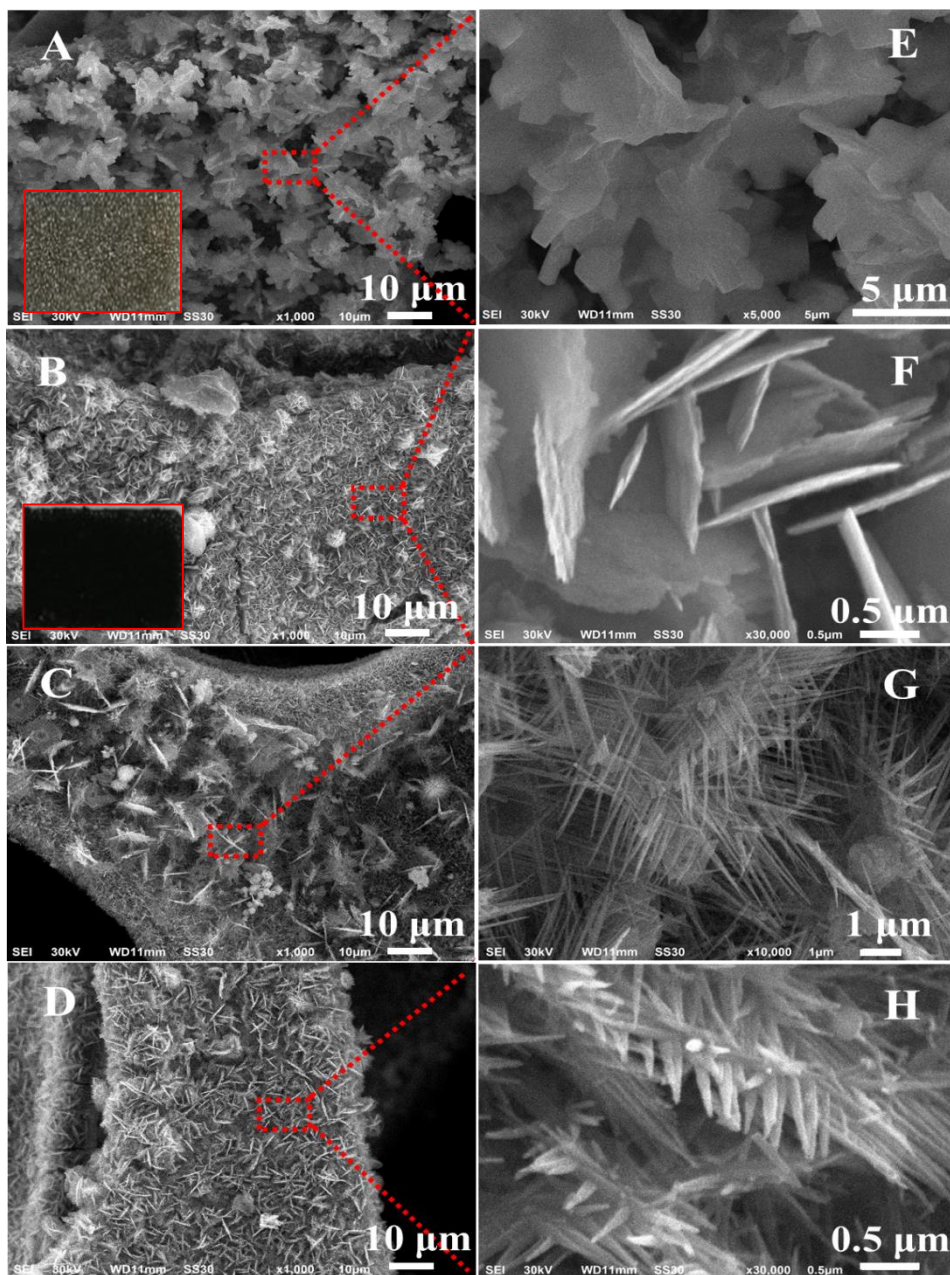


Figure 2. SEM images of the NiCo₂O₄/NF electrode prepared at various reaction times of (A) and (E) 4.0 h, (B) and (F) 6.0 h, (C) and (G) 8.0 h, (D) and (H) 10.0 h. The inset of A and B is the optical photos of pure Ni foam and NiCo₂O₄/NF.

Fig.3 showed the CV curves of NiCo₂O₄/NFs prepared at various reaction times. All NiCo₂O₄/NFs showed two asymmetrical redox peaks at 0.05 V and 0.25 V, which were mainly attributed to the redox reactions of Ni²⁺/Ni and Co⁴⁺/Co [17]. Generally, the electrode with larger CV curve' area shows better electrochemical storage capacity[18]. Here, the NiCo₂O₄/NF (8.0h) showed the largest CV curve' area (in Fig.3A), indicating the highest electrochemical storage capacity comparing to present and previous NiCo₂O₄/NFs[4-5, 15]. The result was attributed to hierarchical micro-structure composed of nanosheets and nanofibers. Fig.3B-E showed the typical CV curves of the NiCo₂O₄/NFs. When the scan rate was improved, the anodic peaks were red shift. The result indicated the low resistance due to

that the NiCo_2O_4 was directly grown on Ni foam [19]. In addition, although the scan rate was improved from 10 to 50 mV s^{-1} , the CV curves still showed obvious redox peaks. These results indicate the good rate performance of $\text{NiCo}_2\text{O}_4/\text{NF}$.

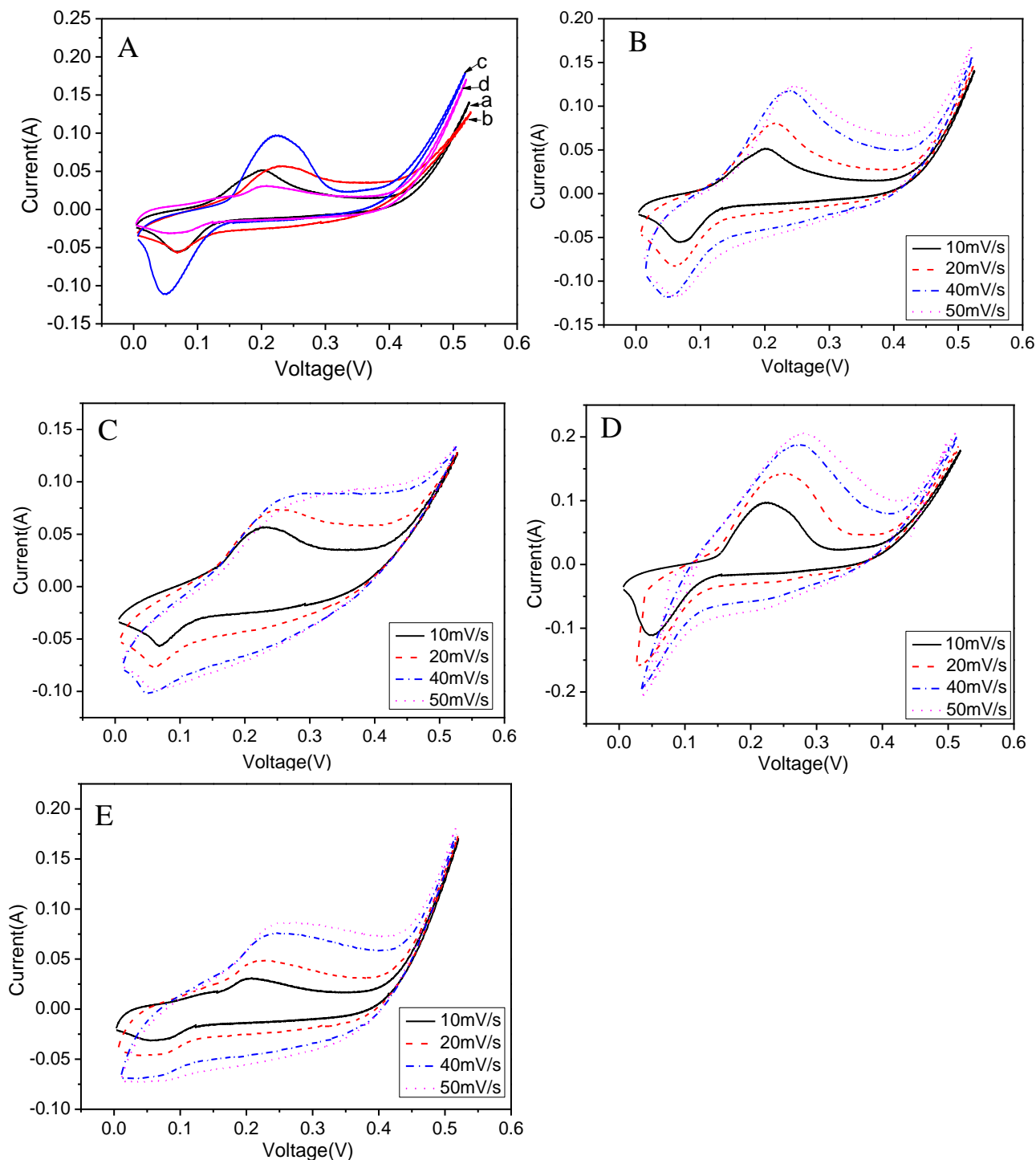


Figure 3. (A) CV curves of the $\text{NiCo}_2\text{O}_4/\text{NFs}$ prepared at various reaction times, (a) 4.0 h, (b) 6.0 h, (c) 8.0 h and (d) 10.0 h. CV curves of $\text{NiCo}_2\text{O}_4/\text{NFs}$ prepared at various reaction times of (B) 4.0 h, (C) 6.0 h, (D) 8.0 h and (E) 10.0 h at various scan rates.

The specific capacitance (C_A) of the NiCo₂O₄/NFs was calculated according to CV curves. The areal capacitance was calculated to be 2.9F cm⁻², 3.5F cm⁻², 4.5F cm⁻² and 3.5F cm⁻² for the NiCo₂O₄/NFs prepared at 4.0 h, 6.0 h, 8.0 h and 10.0 h at a scanning rate of 10.0 mV s⁻¹, respectively (Fig.4A). The areal capacitance of all NiCo₂O₄/NFs decreased with increasing in the scanning rate. However, it still showed large areal capacitance (*ca.* 1.8F cm⁻²) at the scanning rate of 50 mV s⁻¹. The result further confirmed the good rate performance of NiCo₂O₄/NFs. As well-known, the capacitance of electrode strongly depends on its the electrochemical active area (ECSA)[20]. The ECSA was also calculated as shown in Fig.4B. It was about 3.9C cm⁻², 4.5 C cm⁻², 4.7C cm⁻² and 3.5 C cm⁻² for the NiCo₂O₄/NFs prepared at 4.0 h, 6.0 h, 8.0 h and 10.0 h, respectively. The NiCo₂O₄/NF (8.0h) showed a larger ECSA comparing to other NiCo₂O₄/NFs. This result was due to the hierarchical nanofiber array structure of the present NiCo₂O₄/NF. These results also suggested that the NiCo₂O₄/NF (8h) had the best electrochemical performance, resulting in its largest electrochemical active surface area.

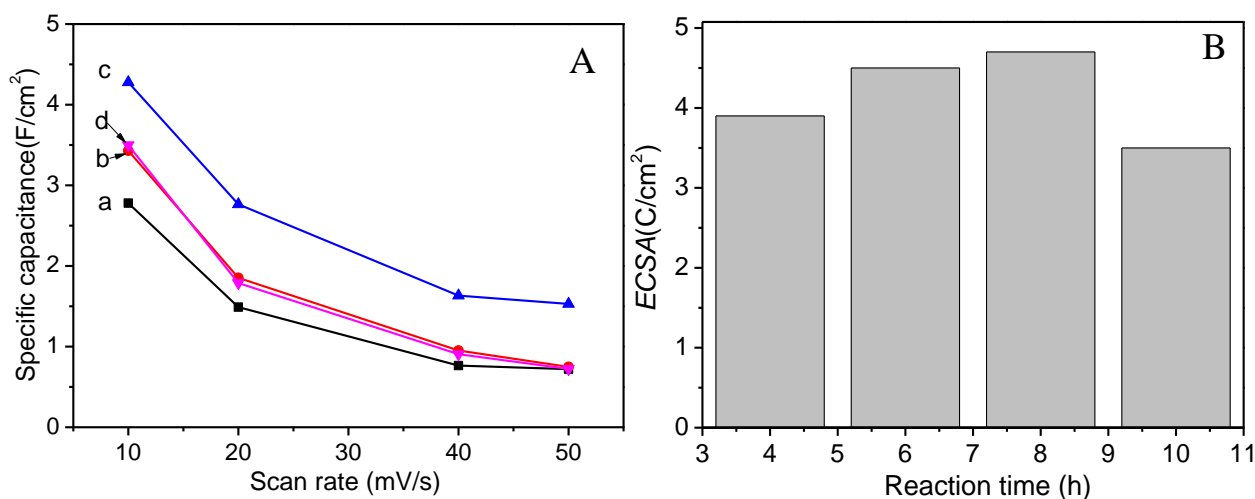


Figure 4. (A) Specific capacitance versus scanning rate of NiCo₂O₄/NFs prepared at various reaction times of (a) 4.0 h, (b) 6.0 h, (c) 8.0 h and (d) 10.0 h. (B) ECSA of the NiCo₂O₄/NFs prepared with various reaction times.

The specific capacitance of NiCo₂O₄/NFs was further characterized by the GCD curves (Fig.5A). The discharge region at the 0.0-0.25V was assigned to the cathodic reaction, indicating a faradaic redox characteristic[21]. Furthermore, the discharge time of the NiCo₂O₄/NF (8.0 h) was the longest, indicating a higher capacitance comparing to other NiCo₂O₄/NFs. The area capacitance was about 2.48F cm⁻², 2.85F cm⁻², 2.89F cm⁻² and 2.81F cm⁻² for the NiCo₂O₄/NFs prepared at 4.0 h, 6.0 h, 8.0 h and 10.0 h, respectively. The GCD curves of the NiCo₂O₄/NF (8.0 h) were also characterized and compared as a function of current density (Fig.5B). The area capacitance of the NiCo₂O₄/NFs was about 2.89F cm⁻², 2.81F cm⁻², 2.83F cm⁻², 2.63F cm⁻² and 2.65F cm⁻² corresponding to a current density of 1.0 mA cm⁻², 2.0 mA cm⁻², 4.0 mA cm⁻² and 5.0 mA cm⁻², respectively. With increasing in current density from 1.0 mA cm⁻² to 5.0 mA cm⁻², the retention of area capacitance was about 94.8%, 91.6%, 91.7% and 90.7% for the NiCo₂O₄/NFs prepared at 4.0 h, 6.0 h, 8.0 h and 10.0 h, respectively (Fig.5C). Fig.5D showed

the cycling stability of the NiCo₂O₄/NFs (8.0h). The area capacitance of the NiCo₂O₄/NF decreased from 2.89F cm⁻² to 2.54F cm⁻² after 2000 cycles. The area capacitance was maintained at about 87.9% of its initial capacity, indicating a stable cyclic life. The excellent cycling stability was attributed the hierarchical structure of NiCo₂O₄ grown on NF. The present NiCo₂O₄/NF exhibited good comprehensive electrochemical performance.

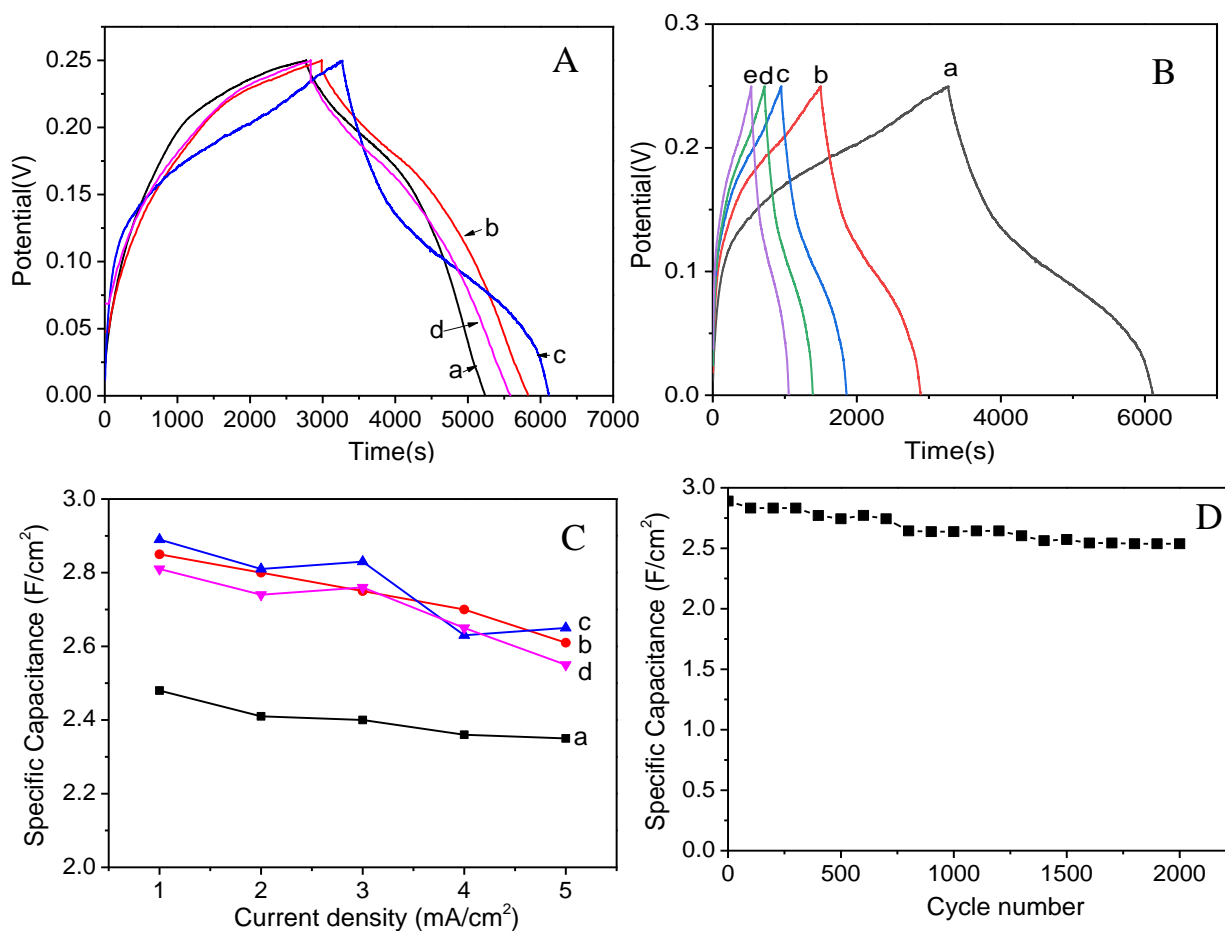


Figure 5. (A) GCD curves of NiCo₂O₄/NFs prepared at various reaction times at a current density of 1.0 mA cm⁻¹, (a) 4.0h, (b) 6.0h, (c) 8.0h and (d) 10.0h. (B) GCD curves of NiCo₂O₄/NF (8h) at various current densities, (a) 1.0 mA cm⁻², (b) 2.0 mA cm⁻², (c) 3.0 mA cm⁻², (d) 4.0 mA cm⁻² and (e) 5.0 mA cm⁻². (C) Specific capacitance versus current density of NiCo₂O₄/NFs prepared at different reaction times of (a) 4.0h, (b) 6.0h, (c) 8.0h and (d) 10.0h. (D) cycling performance of NiCo₂O₄/NF (8.0h).

The mechanism of the NiCo₂O₄/NF with good electrochemical performance was investigated by EIS (Fig.6). The EIS curves of all NiCo₂O₄/NFs were almost straight. The equivalent series resistance (*ESR*) of the NiCo₂O₄/NFs prepared at various reaction times of 4.0 h, 6.0 h, 8.0 h and 10.0 h was about 0.46 Ω, 0.45 Ω, 0.77 Ω and 0.40 Ω, respectively. The low *ESR* indicated a low inner resistance. Furthermore, the present NiCo₂O₄/NFs showed lower inner resistance comparing to other electrodes based on NiCo₂O₄ [4-6, 21]. These results were attributed to the NiCo₂O₄ grown on Ni foam with high electrical conductivity. At the same time, no semicircles were observed, indicating a ultra-low charge-

transfer resistance (R_{ct}) for all NiCo₂O₄/NFs. These results revealed that the present NiCo₂O₄/NFs had low ESR and R_{ct} , which were key factors for achieving good electrochemical storage performance.

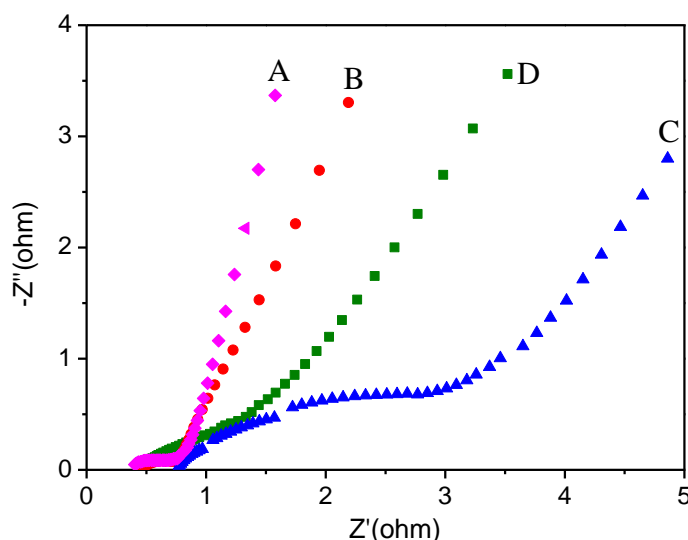


Figure 6. Nyquist plots of NiCo₂O₄/NFs prepared at various reaction times of (A) 4.0 h, (B) 6.0 h, (C) 8.0 h and (D) 10.0 h.

4. CONCLUSIONS

The NiCo₂O₄/NFs with controlled structure have been facily prepared via one-step method. We also found that the structure and electrochemical performance of the NiCo₂O₄/NF strongly depended on the reaction time of NiCo₂O₄ grown on Ni foam. The NiCo₂O₄/NF (8.0 h) showed the largest area capacitance of 4.5F cm⁻² comparing to other NiCo₂O₄/NFs. This result is attributed to the hierarchical and compacting nanofiber array structure, providing larger electrochemical active surface. This study demonstrates a facile method to prepare NiCo₂O₄/NF-based electrode materials with hierarchical porous structure and excellent electrochemical performance for various applications.

ACKNOWLEDGMENTS

The work is grateful for the support from Shanxi Provincial Natural Science Foundation (201803D421081).

References

1. M. Sandhiya, G. Kaviarasan, S. Santhoshkumar and M. Sathish, *New J. Chem.*, 45(2021)21919.
2. C.G. Wang, E. Zhou, W.D. He, X.L. Deng, J.Z. Huang, M. Ding, X.Q. Wei, X.J. Liu and X.J. Xu, *Nanomater.*, 7(2017)41.
3. J.S. Gao, S.L. Li, H.H. Wang, Y. Zhou, L.Y. Zhang, Z.M. Liu and Y.He, *J. Alloys Compd.*, 861 (2021) 157963
4. D.P. Cai, S.H Xiao, D.D. wang, B. Liu, L.L. Wang, Y.Liu, H.Li, Y.R. Wang, Q.H. Li and T.H. Wang, *Electrochim. Acta*, 142 (2014) 118.
5. Q.Y. Zheng, X.Y. Zhang and Y.M. Shen, *Mater. Res. Bull.*, 64(2015)401.

6. Y.Y. Zhang, J.X. Wang, J.H. Ye, P.P. Wan, H.M. Wei, S.Q. Zhao, T.F. Li and S. Hussain, *Ceram. Int.*, 42(2016)14976.
7. R.L. Bai, X.H. Luo, D.S. Zhen, C.G. Ci, J. Zhang, D.W. Wu, M.Q. Cao and Y.L. Liu, *Int. J. Hydrog. Energy*, 45(2020)32343.
8. D.R. Kumar, K.R. Prakasha, A.S. Prakash and J.J. Shim, *J. Alloys Compd.*, 836 (2020)155370.
9. H.Y. Fu, Z.Y. Wang, Y.H. Li and Y. F. Zhang, *Mater. Res. Innovations*, 19(2015)255.
10. Q.W. Zhou, J.C. Xing, Y.F. Gao, X.J. Lv, Y.M. He, Z.H. Guo and Y.M. Li, *ACS Appl. Mater. Interfaces*, 6(2014) 11394.
11. J. Wu, R. Mi, S.M. Li, P. Guo, J. Mei, H. Liu, W.M. Laua and L.M. Liu, *RSC Adv.*, 5(2015)25304.
12. C. Liu, W. Jiang, F.Hu, X. Wu and D.F. Xue, *Inorg. Chem. Front.*, 5(2018),835.
13. C.W.Jia, Y.L.Zhang, Q.Kong, Q.Y.Wang, G.Chen, H.T.Guam and C.J. Dong, *J. Mater. Sci. Mater. Electron.*, 31(2020)6000.
14. Y.You, J.X.Zhao, R.Jiang and J.J. Cao, *Colloid. Polym. Sci.*, 287(2009)839.
15. J. Park, T.H. Ko, S. Balasubramaniam, M.K. Seo, M.S. Khil , H.Y. Kim and B.S. Kim, *Ceram. Int.*, 45(2019)13099.
16. H.J.Yu, Z.Q.Wang, S.L.Yin, C.J.Li, Y.Xu, X.N. Li, L.Wang and H.J.Wang, *ACS Appl. Mater. Interfaces*, 12(2020)436.
17. F. Zhang, C. Su, F.S. Wen, C.P. Mu, X.C. Li, and X.B. Ming, *ChemistrySelect*, 5(2020)2865.
18. T.Han, C.X.Wang, J.R.Yao, J.L.Jin, Y.Y.Sun, Y.H.Zhang and Y.Q.Liu, *Int. J. Electrochem. Sci.*, 12 (2017) 4724.
19. F.Zhang, C.Z. Yuan, X.J.Lu, L.J.Zhang, Q. Che, X.G. Zhang, *J. Power Sources*, 203(2012)250
20. H.Y. Zhang, C.H. Qi, X.J.Du, H. Zhang, Y. Zhang, T.H. Ma, Y.Y.Sun, *Int. J. Hydrog. Energy*, 33(2019)17544.
21. Z.X. Tong, Y.J. Ji, Q.Z. Tian and W.M. Ouyang, *Chem. Commun.*, 55(2019) 9128